

Locally Adaptive Spatial Quantile Smoothing: Application to Monitoring Crime Density in Tokyo

Takahiro Onizuka¹, Shintaro Hashimoto¹ and Shonosuke Sugasawa²

¹Department of Mathematics, Hiroshima University

²Faculty of Economics, Keio University

Abstract

Spatial trend estimation under potential heterogeneity is an important problem to extract spatial characteristics and hazards such as criminal activity. By focusing on quantiles, which provide substantial information on distributions compared with commonly used summary statistics such as means, it is often useful to estimate not only the average trend but also the high (low) risk trend additionally. In this paper, we propose a Bayesian quantile trend filtering method to estimate the non-stationary trend of quantiles on graphs and apply it to crime data in Tokyo between 2013 and 2017. By modeling multiple observation cases, we can estimate the potential heterogeneity of spatial crime trends over multiple years in the application. To induce locally adaptive Bayesian inference on trends, we introduce general shrinkage priors for graph differences. Introducing so-called shadow priors with multivariate distribution for local scale parameters and mixture representation of the asymmetric Laplace distribution, we provide a simple Gibbs sampling algorithm to generate posterior samples. The numerical performance of the proposed method is demonstrated through simulation studies.

Key words: crime data; Markov chain Monte Carlo; Markov random fields; shrinkage prior; spatial trends

1 Introduction

Estimating the spatial trend of the number of crimes is vital to ensure community safety and to respond quickly to incidents. For example, more police may be assigned to areas with a lot of crimes than to areas with few crimes. Tokyo metropolitan police department mentioned that crime predictions have some effects: 1) Efficient development of police officers, 2) Realization of improved public safety, 3) Improving police operations efficiency, 4) Conducting effective patrols. Inference on the crime risk for each area is an important task for crime data analysis, and it has been revealed that crime can be controlled more effectively and efficiently by concentrating police enforcement efforts on high-risk spots and time (e.g. Braga, 2001). Since the number of crimes is often heterogeneous per region, the use of statistical models which take into account such heterogeneity is necessary. In Japan, University of Tsukuba Division of Policy and Planning Sciences Commons provides “GIS database of several police-recorded crimes at O-aza, chome in Tokyo, 2009–2017”. The data contain the number of various crimes from 2009 to 2017 as well as spatial information and the area for each region. Recently, Hamura et al. (2021) and Yano et al. (2021) dealt with the data as zero-inflated count data and they proposed hierarchical Poisson models. It is known that crime data have spatial heterogeneity in the sense that most of the areas have little or no crime throughout multiple years, while others have a lot of crime yearly. Figure 1 shows the averaged values of violent crimes during 2013-2017. The plot indicates that the distribution of violent crimes has spatial heterogeneity and several hotspots. Hamura et al. (2021) regarded the hotspots as outliers and proposed a robust method for violent crimes in 2017. Our goal in this paper is to estimate the spatial high-risk trends of violent crime with uncertainty and to detect the potential risk throughout multiple years simultaneously. It is important to adaptively estimate trends without smoothing for potentially high-risk areas.

Spatial data with longitude and latitude information are considered point-level data. Statistical methods for such data have been developed. As a nonparametric Bayesian approach, Taddy (2010) considered the autoregressive mixture model and also provided

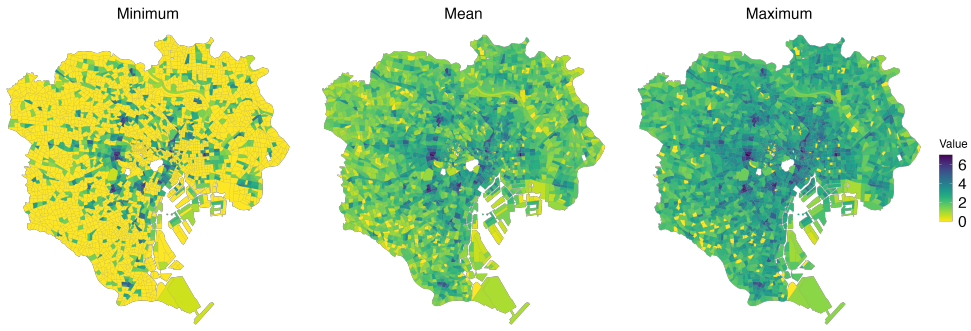


Figure 1: The three values of $\log(1 + Y)$ for crime density Y . From left to right, the minimum, mean, and maximum values for each area over five years from 2013 to 2017.

an application of crime data analysis. On the other hand, data observed per region is known as areal data. Tokyo crime data considered in this paper is also areal data and it is constructed by the total number of crimes per region for a year. In other words, it does not make much sense to consider it as point-level data. For crime data as areal data, Balocchi and Jensen (2019) proposed a Bayesian linear regression model over time within a spatial correlation like conditional autoregressive (CAR) formulation, and they applied their method to an analysis of violent crimes in Philadelphia. For the same data, Balocchi et al. (2019) also proposed the CAR-within-clusters model which assumes linear formulation and conditionally autoregression model for each cluster, which deals with spatial discontinuity by introducing cluster and gives spatial continuity within a cluster. They recommend using the *crime density* defined as the number of crimes divided by the land area to deal with the difference in land size, which makes it seem natural to treat crime data as a continuous value instead of count data. Following the study, we also use the crime density in the Tokyo crime data, and then we assume the continuous distribution on the distribution generating data in our modeling, not count data such as Poisson distribution.

While we focus on trend estimation for spatial data, the smoothing method has been studied in the context of function estimation to investigate the characteristics of the time series data. The ℓ_1 trend filtering (Kim et al., 2009; Tibshirani, 2014) is a nonparametric method to estimate underlying trends, which archives locally adaptive smoothing compared with spline methods, and fast and efficient optimization algorithms

were also proposed (e.g. Ramdas and Tibshirani, 2016). For these reasons, extensions of the original trend filtering have been considered, such as the trend filtering on graphs (Wang et al., 2015) and for functional data (Wakayama and Sugawara, 2021). The Bayesian formulation of trend filtering based on Gaussian likelihood and shrinkage priors has been considered (e.g. Roualdes, 2015; Faulkner and Minin, 2018), and the extension to dynamic shrinkage process is also proposed by Kowal et al. (2019). While these methods focus on mean trends, to estimate quantile trends instead of mean, Brantley et al. (2020) proposed quantile trend filtering, which was compared with the spline method and provides reasonable estimates of the baseline even under the presence of outliers. As the Bayesian methods, Onizuka et al. (2022) and Barata et al. (2022) also proposed the Bayesian quantile trend filtering and the extended dynamic quantile linear model for time series data, respectively.

There are some difficulties with these methods. The main difficulty in applying frequentist trend filtering is that uncertainty quantification is not straightforward. Moreover, the frequentist formulation includes tuning parameters that influence smoothness in the penalty term, but the data-dependent selection of the tuning parameter is not obvious, especially under quantile smoothing. While the Bayesian methods solve these problems, the existing approach suffers only focuses on time series data; thereby it cannot handle the smoothing of data on general graphs such as spatial data. Moreover, most of the studies focused on estimating mean trend under a homogeneous variance structure, and these methods may not work well in data with heterogeneous variance. Nevertheless, quantile smoothing for spatial data has not been studied even a frequentist perspective.

To overcome the issues, we extend the Bayesian quantile smoothing for time series data to Bayesian quantile trend filtering on general graphs including spatial neighboring structures, and also allow for multiple spatial data in which the number of samples for each location may be different. To this end, we employ the asymmetric Laplace distribution as a working likelihood (Yu and Moyeed, 2001), where the theoretical justification of using the likelihood is discussed in Sriram et al. (2013) and Sriram (2015). The novelty of the proposed approach is the construction of the prior distribution on the

graph difference. In particular, we consider the horseshoe prior (Carvalho et al., 2010) as locally adaptive shrinkage priors for the graph differences. We introduce a novel hierarchical formulation for the prior, known as “shadow priors” that enhances the efficiency of posterior computation. Specifically, combining the data augmentation strategy by Kozumi and Kobayashi (2011), we develop a simple Gibbs sampling algorithm to generate posterior samples. We demonstrate the usefulness and wide applicability of proposed methods through extensive simulation studies and application to Tokyo crime data.

The paper is organized as follows: In Section 2, we propose a new Bayesian trend filtering method to estimate quantiles and construct an efficient posterior sampling algorithm based on Gibbs sampling. In Section 3, we illustrate some simulation studies to compare the performance of proposed methods. In Section 4, we apply the proposed methods to crime data in Tokyo as spatial data. Additional numerical results are provided in the Supplementary Material.

2 Bayesian quantile trend filtering on graphs

2.1 Background

Let $y_i = \theta_i + \varepsilon_i$ ($i = 1, \dots, n$) be a sequence model, where y_i is an observation, θ_i is a true function and ε_i is a noise. Let $\hat{\theta}$ be the minimizer of the following penalized problem:

$$\hat{\theta} = \arg \min_{\theta \in \mathbb{R}} \ell(y - \theta) + \lambda \|D^{(k+1)}\theta\|_1, \quad (1)$$

where $\ell(\cdot)$ is a loss function, $y = (y_1, \dots, y_n)^\top$, $\theta = (\theta_1, \dots, \theta_n)^\top$, $D^{(k+1)}$ is a $(n - k - 1) \times n$ difference operator matrix of order $k + 1$, and $\lambda > 0$ is a tuning constant. For $\ell(y - \theta) = \|y - \theta\|_2^2$ in (1), the optimization problem corresponds to ℓ_1 trend filtering (Kim et al., 2009). We note that the ℓ_1 trend filtering is considered as a special case of the generalized lasso proposed by Tibshirani and Taylor (2011). From a computational perspective, Ramdas and Tibshirani (2016) proposed a fast and efficient optimization algorithm to obtain the trend filtering estimate. Depending on the different order k ,

we can express various smoothing such as piecewise constant, linear, quadratic, and so on (Tibshirani, 2014). For spatial data, the trend filtering on graphs was also proposed by Wang et al. (2015) based on the graph difference operator instead of the standard difference operator in (1).

Recently, different loss functions are also considered. For example, Brantley et al. (2020) considered the check loss function $\ell(y - \theta) = \rho_p(y - \theta)$, and proposed quantile trend filtering to estimate the trend in the baseline, not the mean. To solve the problem, Brantley et al. (2020) proposed a parallelizable alternating direction method of multipliers (ADMM) algorithm. Furthermore, they also provided a modified criterion based on the extended Bayesian information criterion to select the tuning parameter.

We next introduce Bayesian trend filtering. In general, the Bayesian formulation for trend filtering is based on the model:

$$y_i = \theta_i + \varepsilon_i, \quad \varepsilon_i \sim f(\cdot), \quad D^{(k+1)}\theta \sim \pi(\cdot), \quad (i = 1, \dots, n), \quad (2)$$

where f and π correspond to the likelihood and prior density functions, respectively. A simple Bayesian counterpart that corresponds to penalized square loss is a combination of the Gaussian likelihood on f and Laplace prior distribution on π (e.g. Roualdes, 2015). The resulting posterior mode is the same as that of the solution of the problem (1). However, it is well-known that the shrinkage based on Laplace prior often causes over-shrinkage due to the tail of Laplace distribution. Recently, Faulkner and Minin (2018) proposed a more flexible Bayesian trend filtering via global-local shrinkage priors such as horseshoe prior (Carvalho et al., 2010). Assuming asymmetric Laplace likelihood in (2), Onizuka et al. (2022) proposed a Bayesian quantile trend filtering. They also provided a calibrated variational Bayes algorithm to reduce the misspecification bias of asymmetric Laplace likelihood. The dynamic quantile linear model based on the extended asymmetric Laplace likelihood is also proposed by Barata et al. (2022).

2.2 Shrinkage priors on graph differences

Following Onizuka et al. (2022), we will consider the following model:

$$y_{ij} = \theta(x_i) + \varepsilon_{ij}, \quad \varepsilon_{ij} \sim \text{AL}(p, \sigma^2), \quad i = 1, \dots, n, \quad j = 1, \dots, N_i, \quad (3)$$

where y_{ij} is a j th observation in the location x_i , $\theta(x_i) = \theta_i$ is a common quantile to y_{i1}, \dots, y_{iN_i} in the location x_i , N_i is the number of data per each location x_i , σ^2 is unknown parameters, and p is a fixed quantile level. Here $\text{AL}(p, \sigma^2)$ denotes the asymmetric Laplace distribution:

$$f_p(x) = \frac{p(1-p)}{\sigma^2} \exp \left\{ -\rho_p \left(\frac{x}{\sigma^2} \right) \right\},$$

where p is a fixed constant which characterizes the quantile level, σ^2 (not σ) is a scale parameter and $\rho_p(\cdot)$ is a check loss function given by

$$\rho_p(r) = \sum_{i=1}^n r_i \{p - 1(r_i < 0)\}, \quad 0 < p < 1.$$

Unlike the standard Bayesian trend filtering model in (2), the model (3) handles the case that there are multiple observations per grid point and assumes that the data is generated as repeated measurements. Note that the assumption seems valid for the crime data considered in this paper as shown in Section 4. It is a natural generalization of the standard trend filtering model for sequence model (see also Heng et al., 2022).

Suppose that spatial location $x = (x_1, \dots, x_n)$ has a graph structure, and then $\theta_1, \dots, \theta_n$ are on general graphs (including the standard trend filtering as a linear chain graph). Following Wang et al. (2015), let $G = (V, E)$ be an undirected graph with vertex set $V = \{1, \dots, n\}$ and edge set E . We assume that $|V| = n$ and $|E| = m$. For $k = 0$, if $e_\ell = (i, j) \in E$, then $D^{(1)}$ has ℓ -th row

$$D_\ell^{(1)} = (0, \dots, 0, \underbrace{1}_i, 0, \dots, 0, \underbrace{-1}_j, 0, \dots, 0), \quad (4)$$

where $1 \leq \ell \leq m$. For a graph G , the graph difference operator of order $k+1$ is denoted

by $D^{(k+1)}$. When $k \geq 1$, graph difference operator $D^{(k+1)}$ is defined by

$$D^{(k+1)} = \begin{cases} (D^{(1)})^\top D^{(k)} & \text{for odd } k, \\ D^{(1)} D^{(k)} & \text{for even } k. \end{cases} \quad (5)$$

Here, we have $D^{(k+1)} \in \mathbb{R}^{n \times n}$ for odd k and $D^{(k+1)} \in \mathbb{R}^{m \times n}$ for even k . We note that the first-order graph difference operator $D^{(1)}$ is a natural generalization of the usual first-order difference operator used in Kim et al. (2009), and if we consider the linear chain graph corresponding to time series data, then they coincide.

Let D be a $m \times n$ full-rank matrix representing a general difference operator on a graph, and we consider flexible shrinkage priors on $D\theta$. When m is smaller than n as in a linear chain graph, D can be transformed to $n \times n$ non-singular matrix (see also Onizuka et al., 2022). We here assume that $m \geq n$ since the number of edges is typically larger than that of nodes. We consider the prior $D\theta \mid \tau^2, \sigma^2, w \sim N_n(0, \tau^2 \sigma^2 W)$ with a diagonal covariance matrix $W = \text{diag}(w_1^2, \dots, w_m^2)$, where $w = (w_1, \dots, w_m)$ represents local shrinkage parameters for each element in $D\theta$ and τ^2 is a global shrinkage parameter. When $m = n$, the prior can be rewritten as

$$\theta \mid \tau^2, \sigma^2, w \sim N_n(0, \sigma^2 \tau^2 (D^\top W^{-1} D)^{-1}).$$

Our idea is to use the above prior form even under $m > n$, noting that the covariance matrix $(D^\top W^{-1} D)^{-1}$ is still non-singular under $m > n$. The density function of the conditional prior of θ is given by

$$\pi(\theta \mid \tau^2, \sigma^2, w) = (2\pi\sigma^2\tau^2)^{-n/2} |D^\top W^{-1} D|^{1/2} \exp\left(-\frac{1}{2\sigma^2\tau^2} \theta^\top D^\top W^{-1} D\theta\right). \quad (6)$$

Now, we consider the prior for w . The standard approach is using an independent prior $\pi(w) = \prod_{i=1}^m \pi(w_i)$, and some familiar distribution is used for $\pi(w_i)$, for example, exponential prior or inverse gamma prior. However, the full conditional distribution of w is not a familiar form due to the term $|D^\top W^{-1} D|^{1/2}$ in the density (6). Alternatively,

we consider the following joint prior:

$$\pi(w) \propto |D^\top W^{-1} D|^{-1/2} |W|^{-1/2} \prod_{i=1}^m \pi(w_i), \quad (7)$$

where $\pi(w_i)$ is a proper univariate distribution. For a square matrix D such that k is odd, the joint prior equals the product of the standard prior $\pi(w_i)$. The prior (7) is a kind of “shadow priors”, and such priors are used to improve the mixing of MCMC (e.g. Liechty et al., 2009) or to construct tractable full conditional distributions (e.g. Liu et al., 2014; Xu and Ghosh, 2015). As shown later, the resulting full conditional distributions of w are familiar forms under well-known priors for local shrinkage parameters.

As univariate distribution $\pi(w_i)$ in (7), we consider two types of distributions, $w_i \sim \text{Exp}(1/2)$ and $w_i \sim C^+(0, 1)$. These priors are motivated from Bayesian lasso prior (Park and Casella, 2008) and horseshoe prior (Carvalho et al., 2010), respectively. Regarding the other parameters, we assign $\sigma^2 \sim \text{IG}(a_\sigma, b_\sigma)$ and $\tau \sim C^+(0, C_\tau)$.

2.3 Markov chain Monte Carlo algorithm

To develop an efficient posterior computation algorithm via Gibbs sampling, we employ the stochastic representation of the asymmetric Laplace distribution (Kozumi and Kobayashi, 2011). For $\varepsilon_{ij} \sim \text{AL}(p, \sigma^2)$, we have the following argumentation

$$\varepsilon_{ij} = \psi z_{ij} + \sqrt{\sigma^2 z_{ij} t^2} u_{ij}, \quad \psi = \frac{1 - 2p}{p(1 - p)}, \quad t^2 = \frac{2}{p(1 - p)},$$

where $u_{ij} \sim N(0, 1)$ and $z_{ij} \mid \sigma^2 \sim \text{Exp}(1/\sigma^2)$ for $i = 1, \dots, n$. From the above expression, the conditional likelihood function of y_{ij} is given by

$$p(y_{ij} \mid \theta_i, z_{ij}, \sigma^2) = (2\pi t^2 \sigma^2)^{-1/2} z_{ij}^{-1/2} \exp \left\{ -\frac{(y_{ij} - \theta_i - \psi z_{ij})^2}{2t^2 \sigma^2 z_{ij}} \right\}.$$

Then, under the conditionally Gaussian prior of θ in (6), the full conditional distributions of z_i and θ are given by

$$\begin{aligned}\theta &| y, z, \sigma^2, \gamma^2 \sim N_n(A^{-1}B, \sigma^2 A^{-1}), \\ z_{ij} &| y_{ij}, \theta_i, \sigma^2 \sim \text{GIG}\left(\frac{1}{2}, \frac{(y_{ij} - \theta_i)^2}{t^2 \sigma^2}, \frac{\psi^2}{t^2 \sigma^2} + \frac{2}{\sigma^2}\right), \quad i = 1, \dots, n, \quad j = 1, \dots, N_i,\end{aligned}$$

where

$$\begin{aligned}A &= \frac{1}{\tau^2} D^\top W^{-1} D + \frac{1}{t^2} \text{diag}\left(\sum_{j=1}^{N_1} z_{1j}^{-1}, \dots, \sum_{j=1}^{N_n} z_{nj}^{-1}\right), \\ B &= \left(\sum_{j=1}^{N_1} \frac{y_{1j} - \psi z_{1j}}{t^2 z_{1j}}, \dots, \sum_{j=1}^{N_n} \frac{y_{nj} - \psi z_{nj}}{t^2 z_{nj}}\right)^\top\end{aligned}$$

and $\text{GIG}(a, b, c)$ denotes the generalized inverse Gaussian distribution. The full conditional distributions of the scale parameter of observations, σ^2 , and global shrinkage parameter τ^2 are given by

$$\begin{aligned}\sigma^2 &| y, \theta, z, w, \tau^2 \sim \text{IG}\left(\frac{n + 3N}{2} + a_\sigma, \beta_{\sigma^2}\right), \\ \tau^2 &| \theta, w, \sigma^2, \xi \sim \text{IG}\left(\frac{n + 1}{2}, \frac{1}{2\sigma^2} \theta^\top D^\top W^{-1} D \theta + \frac{1}{\xi}\right), \quad \xi | \tau^2 \sim \text{IG}\left(\frac{1}{2}, \frac{1}{\tau^2} + 1\right), \\ \beta_{\sigma^2} &= \sum_{i=1}^n \sum_{j=1}^{N_i} \frac{(y_{ij} - \theta_i - \psi z_{ij})^2}{2t^2 z_{ij}} + \frac{\theta^\top D^\top W^{-1} D \theta}{2\tau^2} + \sum_{i=1}^n \sum_{j=1}^{N_i} z_{ij} + b_\sigma,\end{aligned}$$

where N is the number of total data and ξ is an augmented parameter for τ^2 . The full conditional distributions of the other parameters depend on the specific choice of the distributional form of $\pi(w_i)$, which are summarized as follows.

- **(Laplace-type prior)** The full conditional distributions of θ , z_i , and σ^2 have already been mentioned. For Laplace-type prior, we give $\tau^2 = 1$ and $w_i | \gamma^2 \sim \text{Exp}(\gamma^2/2)$. In this condition, we can model that $(D\theta)_i \sim \text{Lap}(\gamma)$. Because our condition is $\gamma \sim C^+(0, 1)$, by using the representation that if $\text{IG}(\gamma^2 | 1/2, 1/\nu)$ and $\text{IG}(\nu | 1/2, 1/a^2)$, then $\gamma \sim C^+(0, a)$, the full conditional distributions of w_i ,

γ^2 and ν are given by

$$w_i^2 \mid \theta, \sigma^2, \gamma^2, \nu \sim \text{GIG} \left(\frac{1}{2}, \frac{\eta_i^2}{\sigma^2}, \gamma^2 \right),$$

$$\gamma^2 \mid w, \nu \sim \text{GIG} \left(m - \frac{1}{2}, \frac{2}{\nu}, \sum_{i=1}^m w_i^2 \right), \quad \nu \mid \gamma^2 \sim \text{IG} \left(\frac{1}{2}, \frac{1}{\gamma^2} + 1 \right),$$

where $\text{GIG}(a, b, c)$ is generalized inverse Gaussian distribution and $\eta_i = (D\theta)_i$.

- **(Horseshoe-type prior)** The full conditional distributions of θ , z_i , σ^2 and τ^2 has already been mentioned. For Horseshoe-type prior, $w_i \sim C^+(0, 1)$. By using the representation that $w_i^2 \mid \nu_i \sim \text{IG}(1/2, 1/\nu_i)$ and $\nu_i \sim (1/2, 1)$, the full conditional distributions of w_i and ν_i are given by

$$w_i^2 \mid \theta, \sigma^2, \gamma^2, \nu \sim \text{IG} \left(1, \frac{1}{\nu_i} + \frac{\eta_i^2}{2\sigma^2\tau^2} \right), \quad \nu_i \mid w_i \sim \text{IG} \left(\frac{1}{2}, \frac{1}{w_i^2} + 1 \right),$$

where $\text{IG}(a, b)$ is inverse Gamma distribution and $\eta_i = (D\theta)_i$.

3 Simulation studies

We illustrate the performance of the proposed method through simulation studies.

3.1 Simulation setting

We show simulation studies for data on 2-D lattice graphs. We formulate the data-generating process as follows. Let $G = (V, E)$ be a 2-D lattice graph. We set $V = \{1, \dots, 100\}$ and $|E| = 180$ for the graph G . The edges are defined by whether the lattice is adjacent or not. We generate noisy data from the model $y_{ij} = f(x_i) + \epsilon(x_i)$ ($i = 1, \dots, 100, j = 1, \dots, 5$), where $x_i = (x_{i1}, x_{i2})$ is a two-dimensional coordinate, and $f(x)$ and $\epsilon(x)$ are a true function and a noise function, respectively. Since we consider the multiple observations situation, we generate five data for each location i . We assume the following two true functions:

- Two block structure

$$f(x_i) = 5 \text{ (center)}, \quad \text{and} \quad f(x_i) = 0 \text{ (other)},$$

- Exponential function

$$f(x_i) = 5 \exp\left(-\frac{1}{2}(x_i - \mu)^\top \Sigma^{-1}(x_i - \mu)\right), \quad \mu = (5.5, 5.5), \quad \Sigma = 3I_2,$$

where $x_i = (x_{i1}, x_{i2})$, $x_{i1}, x_{i2} = 1, 2, \dots, 10$ and I_n is $n \times n$ identity matrix. These functions are shown in Figure 2. As noise functions $\epsilon(x)$, we consider the following three structures:

(I) Homogeneous: $\epsilon(x_i) \sim N(0, 1)$.

(II) Block heterogeneous:

$$\epsilon(x_i) \sim \begin{cases} N(0, 0.5) & (1 \leq x_{i1} \leq 5, 1 \leq x_{i2} \leq 5) \\ N(0, 2) & (6 \leq x_{i1} \leq 10, 6 \leq x_{i2} \leq 10) \\ N(0, 1) & (\text{otherwise}) \end{cases}.$$

(III) Smooth heterogeneous:

$$\epsilon(x_i) \sim \begin{cases} N(0, 0.5) & (1 \leq x_{i1} \leq 4, 1 \leq x_{i2} \leq 4) \\ N(0, 1) & (x_{i1} = 5, 6, 1 \leq x_{i2} \leq 6 \text{ or } 1 \leq x_{i1} \leq 6, x_{i2} = 5, 6) \\ N(0, 1.5) & (x_{i1} = 7, 8, 1 \leq x_{i2} \leq 8 \text{ or } 1 \leq x_{i1} \leq 8, x_{i2} = 7, 8) \\ N(0, 2) & (\text{otherwise}) \end{cases}.$$

The two-block structure is a reasonable function to verify the ability to capture the jump without smoothing. In the exponential function, we examine the ability to estimate a continuous curve with noisy data. The noise (I) represents spatial homogeneity, while the noise may not be realistic in practical situations. In noise (II) and (III), the aim is to verify how well the proposed method can handle spatial heterogeneity. In particular, noise (III) has a stronger degree of spatial heterogeneity than noise (II). The visualizations of these noise distributions are given in Supplementary Materials. Combining two true structures and three noise functions, we consider six scenarios. Scenarios (i), (ii), and (iii) are based on two block structure and noise functions (I), (II), and (III),

respectively. Scenarios (iv), (v), and (vi) are based on exponential structure and noise functions (I), (II), and (III), respectively. Since the noise function is homogeneity, scenarios (i) and (iv) are easier, and scenario (iv) would especially be the easiest because of its smoothness and homogeneity. Scenario (iii) constructed by a two-block structure and smooth heterogeneous noise would be the most difficult for two reasons: hard to capture the jump points and heavy heterogeneity.

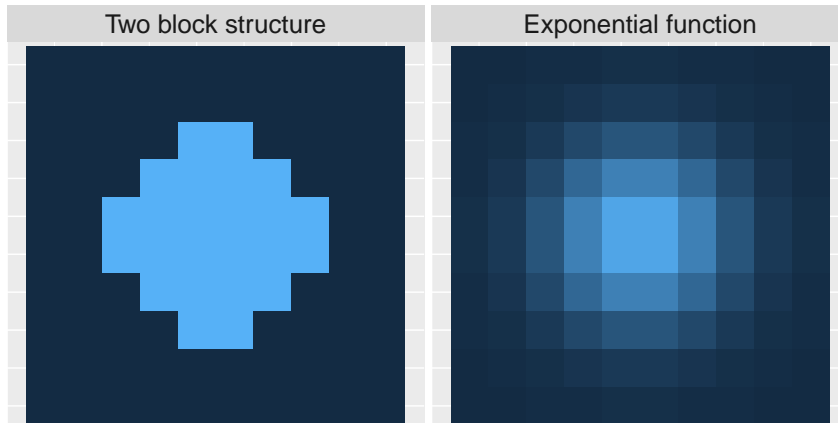


Figure 2: Two types of true function $f(x)$.

We used the two proposed methods (denoted by BQTF-HS and BQTF-Lap), where HS and Lap are the horseshoe and Laplace priors, respectively. Although there is no previous research about spatial quantile smoothing, to evaluate the performance of the proposed method, we compare the BQTF methods with the additive quantile regression (denoted by qgam) which is the frequentist method proposed by Fasiolo et al. (2021). The method can be implemented by using their `qgam` R package. Let $x_i = (x_{i1}, x_{i2})$ be a two-dimensional coordinate where the data y_i is observed, and then qgam estimate $\hat{\theta}_i$ is composed of the sum of functions such as $\hat{\theta}_i = \hat{q}_1(x_{i1}) + \hat{q}_2(x_{i2})$ where $\hat{q}_1(\cdot)$ and $\hat{q}_2(\cdot)$ are nonparameteric quantile functions. If the data y_i is generated from a simple true function $f(x_i) = f_1(x_{i1}) + f_2(x_{i2})$, then the qgam method would give a pretty good smoothing, but it is unrealistic in a practical situation and the simulation setting is more complicated. For the proposed methods, we generated 7500 posterior samples, and then only every 10th scan was saved, and the order of trend filtering is set as $k = 1$ (i.e. area-wise linear trend). We estimate five quantile levels: 0.1, 0.3, 0.5, 0.7, and 0.9.

To evaluate the performance of estimates, we adopt the mean squared error (MSE), the mean absolute deviation (MAD), the mean credible interval width (MCIW), and the coverage probability (CP) which are defined by

$$\begin{aligned} \text{MSE} &= \frac{1}{n} \sum_{i=1}^n (\theta_i^* - \hat{\theta}_i)^2, & \text{MAD} &= \frac{1}{n} \sum_{i=1}^n |\theta_i^* - \hat{\theta}_i|, \\ \text{MCIW} &= \frac{1}{n} \sum_{i=1}^n \hat{\theta}_{97.5,i} - \hat{\theta}_{2.5,i}, & \text{CP} &= \frac{1}{n} \sum_{i=1}^n I(\hat{\theta}_{2.5,i} \leq \theta_i^* \leq \hat{\theta}_{97.5,i}), \end{aligned}$$

respectively, where $\hat{\theta}_{100(1-\alpha),i}$ represent the $100(1 - \alpha)\%$ posterior quantiles of θ_i and θ_i^* are true quantiles at location x_i . These values were averaged over 100 replications of simulating datasets.

3.2 Simulation result

Simulation results are shown in Tables 1 and 2. Note that MCIW and CP are reported only for Bayesian methods. From Tables 1 and 2, the proposed BQTF method under horseshoe prior tends to provide a reasonable point estimate not only in the case of homogeneous but also for heterogeneous variances. When the true structure is the exponential function (such as scenarios (iv), (v), and (vi)), the proposed two methods provide comparable point estimates, and the additive quantile regression has smaller MSE and MAD than that for (i), (ii) and (iii) scenarios. However, it is observed that the additive quantile regression does not work well for any scenario compared with the proposed methods. In terms of uncertainty quantification, while BQTF methods have reasonable coverage probabilities for the 50% quantile trend, the coverage probabilities of 95% credible intervals for extremal quantiles such as 0.1 and 0.9 seem to be far away from the nominal coverage rate of 0.95.

4 Application to crime trend analysis in Tokyo

We apply the proposed methods to spatial data analysis. We used the ‘‘GIS database of number of police-recorded crime at O-aza, chome in Tokyo, 2009–2017’’, which was provided by University of Tsukuba Division of Policy and Planning Sciences Commons.

Table 1: Average values of MSE and MAD based on 100 replications for scenarios (i), (ii), and (iii) (two-block structure). The minimum values of MSE and MAD are represented in bold.

Scenario (i)										
	MSE					MAD				
	0.1	0.3	0.5	0.7	0.9	0.1	0.3	0.5	0.7	0.9
BQTF-HS	0.264	0.157	0.138	0.152	0.249	0.377	0.282	0.265	0.281	0.371
BQTF-Lap	0.337	0.212	0.193	0.211	0.339	0.460	0.359	0.344	0.360	0.463
qgam	3.985	2.461	1.877	2.269	3.062	1.256	1.266	1.195	1.266	1.425
	MCIW					CP				
	0.1	0.3	0.5	0.7	0.9	0.1	0.3	0.5	0.7	0.9
BQTF-HS	1.322	1.289	1.259	1.262	1.286	0.824	0.918	0.933	0.919	0.827
BQTF-Lap	1.402	1.554	1.552	1.542	1.393	0.801	0.910	0.923	0.907	0.800
Scenario (ii)										
	MSE					MAD				
	0.1	0.3	0.5	0.7	0.9	0.1	0.3	0.5	0.7	0.9
BQTF-HS	0.465	0.271	0.243	0.256	0.451	0.454	0.337	0.316	0.329	0.448
BQTF-Lap	0.541	0.311	0.283	0.307	0.541	0.524	0.400	0.381	0.400	0.526
qgam	3.973	2.419	1.891	2.219	3.208	1.315	1.241	1.197	1.256	1.459
	MCIW					CP				
	0.1	0.3	0.5	0.7	0.9	0.1	0.3	0.5	0.7	0.9
BQTF-HS	1.432	1.410	1.367	1.379	1.386	0.816	0.911	0.920	0.908	0.814
BQTF-Lap	1.544	1.689	1.676	1.677	1.526	0.802	0.906	0.918	0.909	0.797
Scenario (iii)										
	MSE					MAD				
	0.1	0.3	0.5	0.7	0.9	0.1	0.3	0.5	0.7	0.9
BQTF-HS	0.649	0.395	0.346	0.375	0.603	0.580	0.438	0.408	0.426	0.559
BQTF-Lap	0.739	0.431	0.390	0.424	0.740	0.643	0.492	0.470	0.488	0.642
qgam	3.792	2.295	1.908	2.174	2.984	1.366	1.258	1.204	1.255	1.422
	MCIW					CP				
	0.1	0.3	0.5	0.7	0.9	0.1	0.3	0.5	0.7	0.9
BQTF-HS	1.810	1.799	1.767	1.764	1.782	0.795	0.898	0.912	0.898	0.805
BQTF-Lap	1.930	2.077	2.063	2.062	1.908	0.791	0.900	0.917	0.900	0.791

Table 2: Average values of MSE and MAD based on 100 replications for scenarios (iv), (v), and (vi) (exponential function). The minimum values of MSE and MAD are represented in bold.

	Scenario (iv)									
	MSE					MAD				
	0.1	0.3	0.5	0.7	0.9	0.1	0.3	0.5	0.7	0.9
BQTF-HS	0.135	0.082	0.075	0.081	0.135	0.280	0.218	0.208	0.214	0.274
BQTF-Lap	0.183	0.082	0.072	0.082	0.186	0.341	0.224	0.212	0.226	0.342
qgam	0.577	0.450	0.387	0.418	0.510	0.522	0.503	0.504	0.522	0.551
	MCIW					CP				
BQTF-HS	0.992	0.983	0.983	0.984	1.022	0.817	0.907	0.919	0.911	0.847
BQTF-Lap	1.160	1.148	1.137	1.143	1.169	0.857	0.953	0.963	0.953	0.863
	Scenario (v)									
	MSE					MAD				
	0.1	0.3	0.5	0.7	0.9	0.1	0.3	0.5	0.7	0.9
BQTF-HS	0.283	0.126	0.109	0.123	0.281	0.355	0.246	0.228	0.242	0.348
BQTF-Lap	0.312	0.116	0.095	0.115	0.312	0.396	0.247	0.225	0.246	0.396
qgam	0.686	0.472	0.398	0.432	0.619	0.588	0.515	0.508	0.527	0.601
	MCIW					CP				
	0.1	0.3	0.5	0.7	0.9	0.1	0.3	0.5	0.7	0.9
BQTF-HS	1.140	1.076	1.068	1.081	1.154	0.814	0.909	0.928	0.913	0.830
BQTF-Lap	1.308	1.227	1.207	1.225	1.302	0.849	0.945	0.960	0.946	0.852
	Scenario (vi)									
	MSE					MAD				
	0.1	0.3	0.5	0.7	0.9	0.1	0.3	0.5	0.7	0.9
BQTF-HS	0.350	0.169	0.142	0.152	0.314	0.424	0.305	0.279	0.288	0.402
BQTF-Lap	0.435	0.170	0.140	0.157	0.406	0.487	0.307	0.280	0.296	0.469
qgam	0.916	0.598	0.492	0.505	0.655	0.718	0.592	0.565	0.579	0.660
	MCIW					CP				
	0.1	0.3	0.5	0.7	0.9	0.1	0.3	0.5	0.7	0.9
BQTF-HS	1.388	1.295	1.274	1.271	1.415	0.797	0.889	0.911	0.900	0.832
BQTF-Lap	1.634	1.520	1.476	1.484	1.611	0.836	0.939	0.953	0.942	0.852

The data contains the number of crimes in Tokyo, and we focus on the violent crime data in particular. We used the number of violent crimes at from some 23 wards in Tokyo for five years (from 2013 to 2017) whose number of locations is $n = 3,125$ and the sample size is $N = 3125 \times 5 = 15,625$. The number of edges is 9000. The edges are constructed based on the 5 nearest neighbor searches. Namely, when x_j is in 5 nearest neighbors of x_i , then we connect x_i and x_j even if they are not adjacent to each other on the map. Since the data also involve information on the area (km^2) of each region, we define $Y = (Y_1, \dots, Y_{3125})$ as the values of the number of violent crimes divided by the area for each region, which are called *crime density* as we mentioned in Section 1. Using the value of Y may be reasonable because the larger the area, the greater the number of crimes in general. Balocchi et al. (2019) also used the crime density normalized by the area. Moreover, we use the value on the log scale as data $y = \log(1+Y)$. Such a transformation is popular in the literature (see also Balocchi and Jensen, 2019). We regard five years of data as multiple observation data per location. The data is shown in Figure 3, and the plot indicates that spatial trends have not changed over the years. In addition, the histograms of y for each year and all years are also shown in Figure 4, which represent that the distribution of observed data is the same for all years. While there are some hotspots for each year in Figure 3, some high-risk areas have overlapped throughout the five years. They tend to be particularly common in downtown areas, and such areas can be seen as ones with potentially high risk. In this section, our goal is to estimate spatial quantile trends and detect potential hotspots. In particular, since we are interested in the median and high-risk cases of criminal activity, we estimate 50% and 90% quantile trends. We adopt the proposed Bayesian quantile trend filtering under horseshoe prior (BQTF-HS) and compare the performance with the additive quantile regression (qgam) using latitude and longitude as covariates. For the proposed method, we generated 50,000 posterior samples, and then the first 10000 samples are discarded and only every 40th scan was saved. The order of trend filtering is $k = 1$. The estimated quantile trends are shown in Figure 5. Note that if the estimate has a negative value, then it is plotted as zero. The proposed BQTF method seems to capture the zero-inflated data throughout five years. For the

90% quantile trend, the BQTF method provides more adaptive smoothing that detects not only high-risk spots but also low-risk spots and gives smoothing a high quantile trend. On the other hand, the additive quantile regression (qgam) method results in over-shrinkage and clearly can not achieve a locally adaptive smoothing. In other words, the qgam method can not detect hotspots, and the areas that seem to be not hotspots also have a green or blue color. Hence, the BQTF method provides a locally adaptive smoothing for high quantile trends and captures latent heterogeneity by treating five years of data as multiple observations.

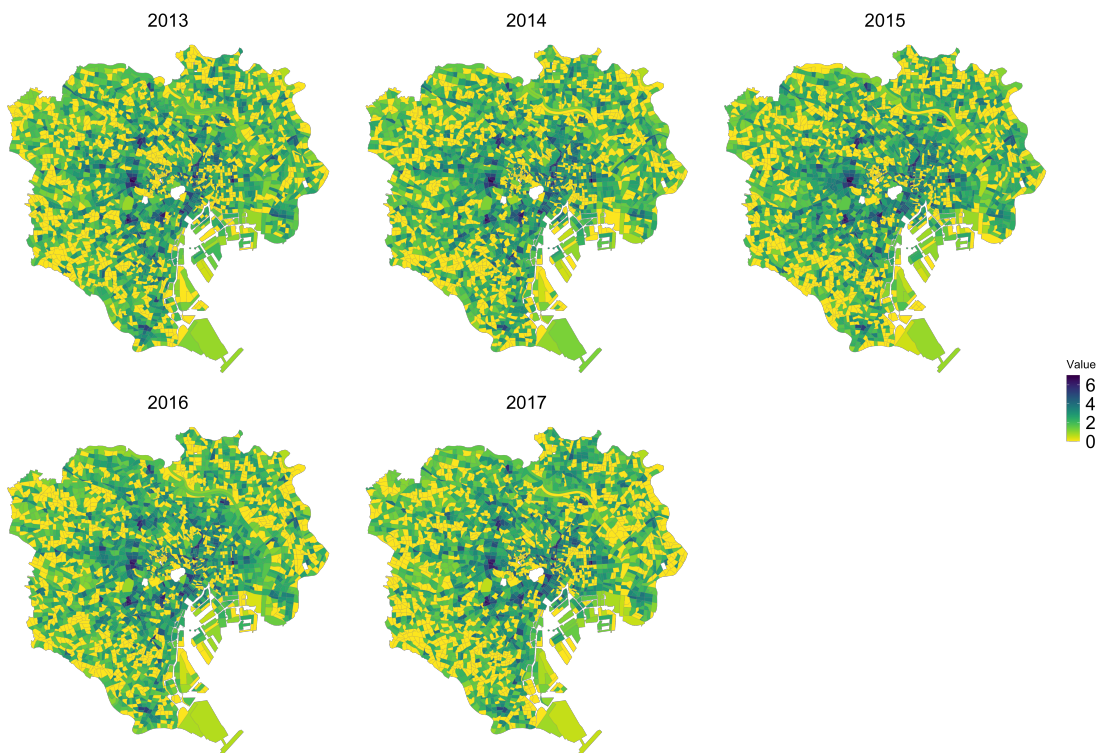


Figure 3: The values of $\log(1 + Y)$ for crime density Y from 2013 to 2017.

5 Discussion

In this paper, we proposed a Bayesian quantile trend filtering (BQTF) method on graphs under continuous shrinkage priors, which enables us to estimate quantile trends for spatial data. We also provide a simple Gibbs sampler by introducing a kind of shadow prior. Through simulation studies, it is shown that the BQTF estimates under

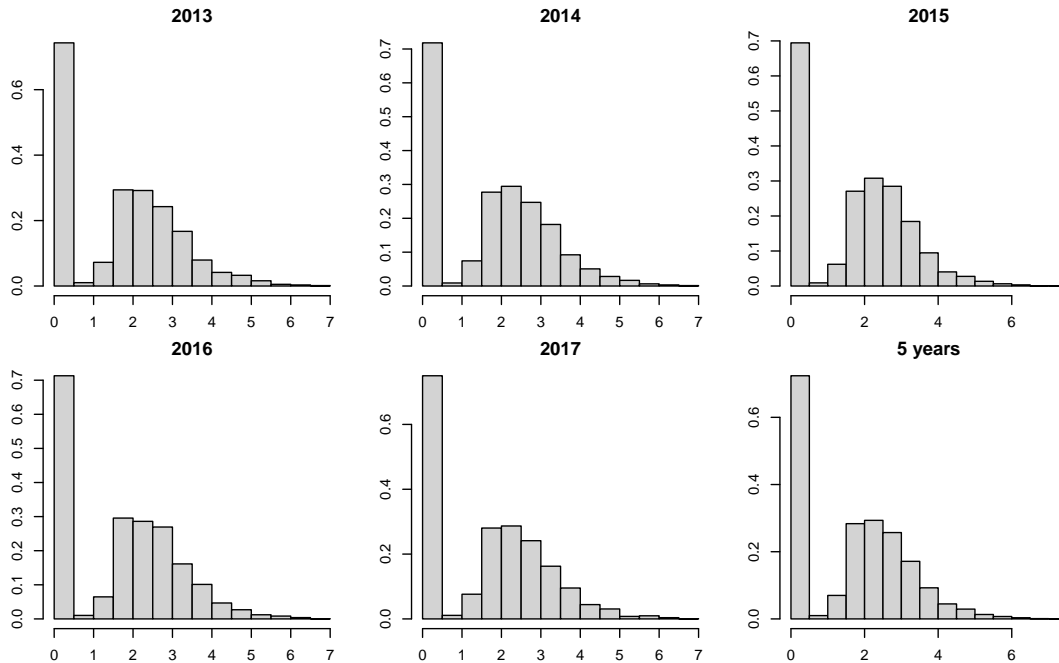


Figure 4: The histogram of the crime densities for each year and five-year data.

the horseshoe prior provide more locally adaptive smoothing of the quantile trend than the other methods. The application of the violent crime data in Tokyo gives interesting results in that the proposed method provides locally adaptive quantile smoothing for all quantiles and detects hotspots focusing on a low quantile level.

There are several future directions for this paper. First, it should be proved some theoretical results for Bayesian quantile trend filtering such as the posterior consistency under misspecified asymmetric Laplace likelihood, the valid uncertainly quantification, and the posterior contraction rate (see also Sriram et al., 2013; Sriram, 2015; Banerjee, 2021). Furthermore, since the proposed methods do not work well to estimate extremal quantiles, it is also important to extend the proposed methods to smoothing for extremal quantiles (e.g. Chernozhukov, 2005). In terms of application, while we use areal data, the trend estimation of point-level data has also been studied (see also Lum and Gelfand, 2012). Since the observation points of these data are different between years, the proposed methods cannot be used as is to detect potential hotspots throughout multiple years.

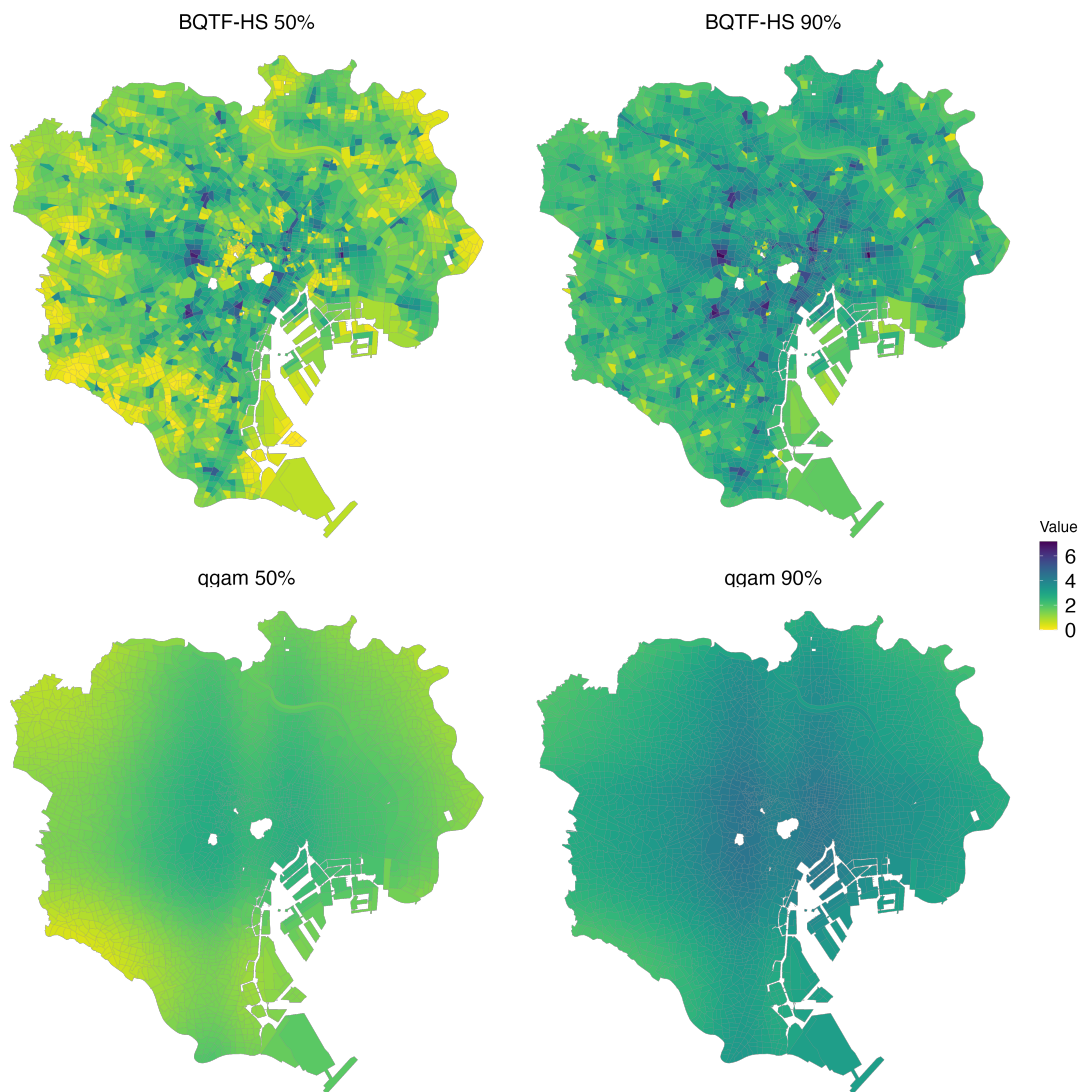


Figure 5: Estimated trends via BQTF-HS (top) and qqam (bottom) for two quantile levels: 50% (left) and 90% (right).

Acknowledgement

This work is supported by JST, the establishment of university fellowships towards the creation of science technology innovation, Grant Number JPMJFS2129. This work is partially supported by Japan Society for Promotion of Science (KAKENHI) grant numbers 21K13835 and 21H00699.

References

- Balocchi, C., S. K. Deshpande, E. I. George, and S. T. Jensen (2019). Crime in philadelphia: Bayesian clustering with particle optimization. *arXiv preprint arXiv:1912.00111*.
- Balocchi, C. and S. T. Jensen (2019). Spatial modeling of trends in crime over time in philadelphia. *The Annals of Applied Statistics* 13(4), 2235–2259.
- Banerjee, S. (2021). Horseshoe shrinkage methods for bayesian fusion estimation. *arXiv preprint arXiv:2102.07378*.
- Barata, R., R. Prado, and B. Sansó (2022). Fast inference for time-varying quantiles via flexible dynamic models with application to the characterization of atmospheric rivers. *The Annals of Applied Statistics* 16(1), 247–271.
- Braga, A. A. (2001). The effects of hot spots policing on crime. *The Annals of the American Academy of Political and Social Science* 578(1), 104–125.
- Brantley, H. L., J. Guinness, and E. C. Chi (2020). Baseline drift estimation for air quality data using quantile trend filtering. *The Annals of Applied Statistics* 14(2), 585–604.
- Carvalho, C. M., N. G. Polson, and J. G. Scott (2010). The horseshoe estimator for sparse signals. *Biometrika* 97(2), 465–480.
- Chernozhukov, V. (2005). Extremal quantile regression. *The Annals of Statistics* 33(2), 806–839.

- Fasiolo, M., S. N. Wood, M. Zaffran, R. Nedellec, and Y. Goude (2021). Fast calibrated additive quantile regression. *Journal of the American Statistical Association* 116(535), 1402–1412.
- Faulkner, J. R. and V. N. Minin (2018). Locally adaptive smoothing with markov random fields and shrinkage priors. *Bayesian analysis* 13(1), 225.
- Hamura, Y., K. Irie, and S. Sugasawa (2021). Robust hierarchical modeling of counts under zero-inflation and outliers. *arXiv preprint arXiv:2106.10503*.
- Heng, Q., H. Zhou, and E. C. Chi (2022). Bayesian trend filtering via proximal markov chain monte carlo. *arXiv preprint arXiv:2201.00092*.
- Kim, S.-J., K. Koh, S. Boyd, and D. Gorinevsky (2009). ℓ_1 trend filtering. *SIAM review* 51(2), 339–360.
- Kowal, D. R., D. S. Matteson, and D. Ruppert (2019). Dynamic shrinkage processes. *Journal of the Royal Statistical Society: Series B (Statistical Methodology)* 81(4), 781–804.
- Kozumi, H. and G. Kobayashi (2011). Gibbs sampling methods for bayesian quantile regression. *Journal of Statistical Computation and Simulation* 81(11), 1565–1578.
- Liechty, M. W., J. C. Liechty, and P. Müller (2009). The shadow prior. *Journal of Computational and Graphical Statistics* 18(2), 368–383.
- Liu, F., S. Chakraborty, F. Li, Y. Liu, and A. C. Lozano (2014). Bayesian regularization via graph laplacian. *Bayesian Analysis* 9(2), 449–474.
- Lum, K. and A. E. Gelfand (2012). Spatial quantile multiple regression using the asymmetric laplace process. *Bayesian Analysis* 7(2), 235–258.
- Onizuka, T., S. Hashimoto, and S. Sugasawa (2022). Fast and locally adaptive bayesian quantile smoothing using calibrated variational approximations. *arXiv preprint arXiv:2211.04666*.

- Park, T. and G. Casella (2008). The bayesian lasso. *Journal of the American Statistical Association* 103(482), 681–686.
- Ramdas, A. and R. J. Tibshirani (2016). Fast and flexible admm algorithms for trend filtering. *Journal of Computational and Graphical Statistics* 25(3), 839–858.
- Roualdes, E. A. (2015). Bayesian trend filtering. *arXiv preprint arXiv:1505.07710*.
- Sriram, K. (2015). A sandwich likelihood correction for bayesian quantile regression based on the misspecified asymmetric laplace density. *Statistics & Probability Letters* 107, 18–26.
- Sriram, K., R. Ramamoorthi, and P. Ghosh (2013). Posterior consistency of bayesian quantile regression based on the misspecified asymmetric laplace density. *Bayesian Analysis* 8(2), 479–504.
- Taddy, M. A. (2010). Autoregressive mixture models for dynamic spatial poisson processes: Application to tracking intensity of violent crime. *Journal of the American Statistical Association* 105(492), 1403–1417.
- Tibshirani, R. J. (2014). Adaptive piecewise polynomial estimation via trend filtering. *The Annals of statistics* 42(1), 285–323.
- Tibshirani, R. J. and J. Taylor (2011). The solution path of the generalized lasso. *The Annals of Statistics* 39(3), 1335–1371.
- Wakayama, T. and S. Sugawara (2021). Locally adaptive smoothing for functional data. *arXiv preprint arXiv:2104.02456*.
- Wang, Y.-X., J. Sharpnack, A. Smola, and R. Tibshirani (2015). Trend filtering on graphs. In *Artificial Intelligence and Statistics*, pp. 1042–1050. PMLR.
- Xu, X. and M. Ghosh (2015). Bayesian variable selection and estimation for group lasso. *Bayesian Analysis* 10(4), 909–936.
- Yano, K., R. Kaneko, and F. Komaki (2021). Minimax predictive density for sparse count data. *Bernoulli* 27(2), 1212–1238.

Yu, K. and R. A. Moyeed (2001). Bayesian quantile regression. *Statistics & Probability Letters* 54(4), 437–447.

Supplementary Materials for “Locally Adaptive Spatial Quantile Smoothing: Application to Monitoring Crime Density in Tokyo”

This Supplementary Material provides additional information for the simulation study and sample paths of the MCMC algorithm applied to Tokyo crime data.

S1 Additional information for simulation study

Figure S1 summarizes the plot of true five quantile trends under three noise distribution ϵ in the simulation study (see also Section 3). We considered the three scenarios: that is (I) homogeneous, (II) block heterogeneous, and (III) smooth heterogeneous.

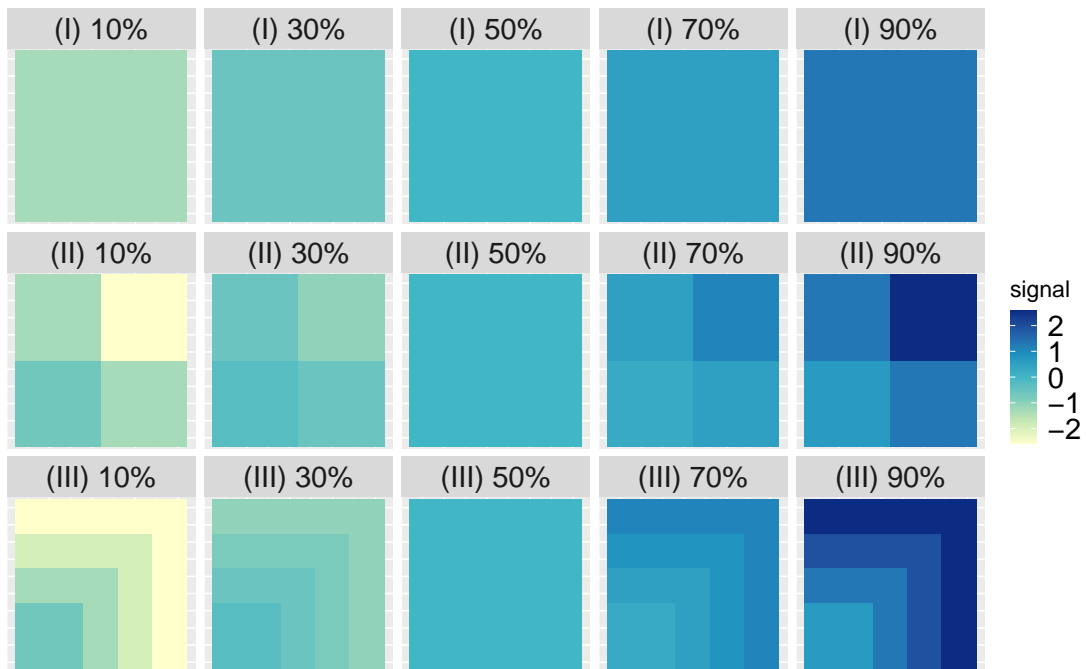


Figure S1: The true p -th quantiles ($p = 0.1, 0.3, 0.5, 0.7, 0.9$) for three noise distributions from top to bottom: (I), (II), (III).

S2 Sampling efficiency of the MCMC algorithm for Tokyo crime data

We confirm that the proposed algorithm works well by making a simple diagnosis of sampling efficiency. Here, we especially consider the sampling efficiency in the analysis of Tokyo crime data. We use the same posterior samples in Section 4, that is, every 20th value of θ_i from a Markov chain of length 50,000. Sample paths and autocorrelations of the posterior samples in six selected areas are provided in Figures S2. Mixing of the proposed algorithm is reasonable, and autocorrelations rapidly decay.

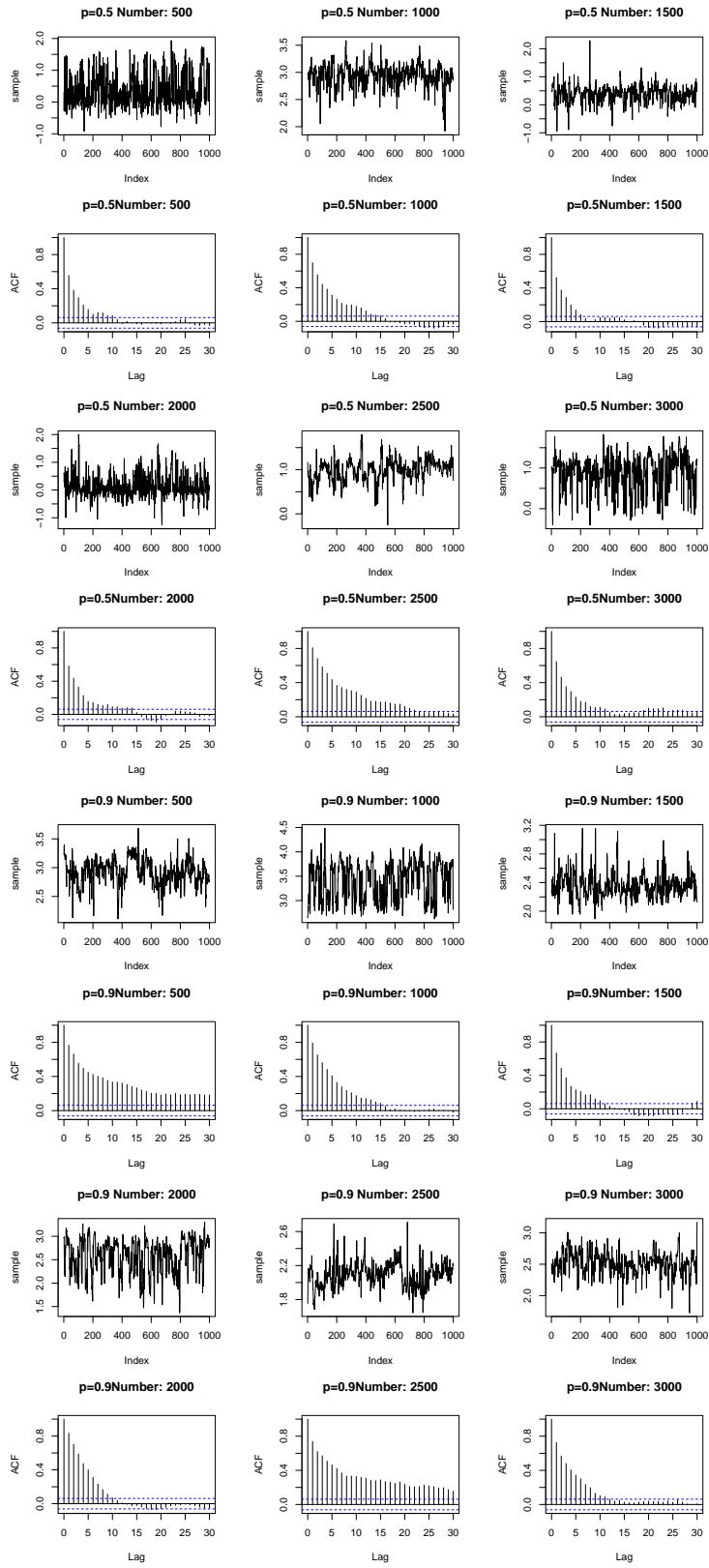


Figure S2: Sample paths and autocorrelations of the posterior samples of θ_i of BQTF in six areas under horseshoe prior applied to Tokyo crime data.